Wasit Journal for Pure Science

Journal Homepage: https://wjps.uowasit.edu.iq/index.php/wjps/index
e-ISSN: 2790-5241 p-ISSN: 2790-5233

Efficient Numerical Solution of the Sharma-Tasso-Olver Equation Using Radial Basis Function-Pseudo Spectral Method with Comparative Analysis

Mardan A. Pirdawood[1], Luqman M. Yaseen[2]*, Mohammed I. Sadeeq[3], Bashdar O. Hussen[4], Twana A. Ali[5], Yad A. Kareem[6],

[1,4,5,6]Koya University, Department of Mathematics, Faculty of Science and Health, IRAQ

[2,3]Akre University for Applied Sciences, Department of Mathematics, College of education, RAQ

*Corresponding Author: Luqman M. Yaseen

DOI: https://doi.org/10.31185/wjps.335
Received 02 March 2024; Accepted 02 April 2024; Available online 30 Jun 2024

ABSTRACT: In this study, we will solve the Sharma-Tasso-Olver equation by utilizing the radial basis function-pseudo spectral approach. Pseudo spectral techniques are renowned for their exceptional precision but have constraints regarding their ability to handle geometric variations. The integration of Radial Basis Functions (RBF) with pseudo spectral methods offers a solution to surmount this particular limitation. To estimate the differentials with respect to the variable x, we will use the radial basis functions, including commonly used ones like multiquadric, inverse multiquadric, and inverse quadric, have been employed. Furthermore, the problem has transformed into the ordinary differential equation (ODE), and the solution to this ODE system has been acquired through the application of the fourth-order Runge-Kutta method. Additionally, a comparative analysis has been conducted between the solutions obtained through the suggested technique and the exact solutions.

Keywords: Sharma-Tasso-Olver equation, Radial basis functions pseudo spectral method, Runge-Kutta fourth order method.

1. INTRODUCTION

The Sharma-Tasso-Olver (STO) model is a nonlinear partial differential equation within Burger's hierarchy, employed to depict the processes of fission fusion and solitary waves in scientific and engineering realms such as nonlinear optics, plasma and quantum physics. The generalized STO equation will have the following formula (Zhou and Zhuang, 2022):

$$v_t + \beta(v^3)_x + \frac{3}{2}\beta(v^2)_{xx} + \beta v_{xxx} = 0, \tag{1}$$

The function $v(x,t)$ is dependent on variables x and t, where β is a non-zero parameter, x is for spatial and t is for temporal. Nonlinear partial differential equations (PDEs) serve as a valuable tool for describing various physical characteristics and traits associated with nonlinear complex events. Investigating solutions for these nonlinear PDEs is a crucial focus for researchers, as it provides deeper insights into the interpretation of dynamic processes and nonlinear physical phenomena. Recent years have witnessed significant progress in algorithmic techniques and their applications within this field. Numerous effective methods and modifications have been developed and applied to address the challenges posed by nonlinear partial differential equations, contributing to advancements in the understanding and analysis of these complex systems.

In the study conducted by (Wazwaz, 2007), the analytical examination of the STO problem involved the successful application of the tan hyperbolic also its extension techniques, along with extra assumptions incorporating exponential and hyperbolic functions. The exploration of solitary traveling waves and periodic for the equation employed an improved

*Corresponding author: luqman.mahmood@auas.edu.krd

G'/G-expansion method recommended by (He, et al. 2013). For the STO equation, the investigation further utilized fractional derivatives, including the modified Riemann-Liouville derivative, to derive its an exact solution as demonstrated by (Uddin, et al. 2019).

The original methodology employed in generating unique exact traveling wave solutions for the STO equation involved utilizing Kudryashov expansion's generalization, the introduction of the extended F-expansion and novel sub-equations. This approach accommodated variable coefficients within the STO equation. The innovative solutions emerged through the application of rational functions, as detailed in the work by (Abdou, et al. 2020). Additionally, a 3-wave method was represented for the (3+1)-dimensional STO-like model, employing the homoclinic methodology. This resulted in the identification of diverse solution types for the STO equation, incorporating various random parameters, as elucidated in the study by (Kang, et al. 2019). In the resolution of nonlinear partial differential equations (PDEs), advanced techniques were employed by (Sabawi, et al. 2021 & Pirdawood and Sabawi, 2021), utilizing high-order compact finite difference methods. Meanwhile, (Zhou and Zhuang, 2022) addressed traveling equations associated with a cubic oscillator incorporating damping effects. This oscillator exhibited both time-independent and time-dependent first integrals, enabling the derivation of precise explicit kink wave solutions for all restricted orbits within the traveling system. Additionally, in the study was done by (Sheikh, et al. 2023) they employed the Extended Mapping Spectral Element (EMSE) approach to generalize solitary wave solutions for the Soliton (STO) equation.

In this paper, we utilize radial basis functions (RBFs) to estimate space derivatives, presenting them as a viable substitute for conventional methods. RBFs have gained increasing prominence in approximating solutions for partial differential equations (PDEs). The application of RBFs to solve PDEs was initially introduced by Kansa in 1990, who employed the multi-quadric RBF to provide an approximate solution for diverse forms of PDE systems (Buhmann, 2000).

The Radial Basis Function-Pseudo Spectral (RBF-PS) method is a numerical method for solving PDEs. A practical and robust semi-discrete technique known as the RBF-PS approach is utilized. In accordance with this method, the original partial differential equation undergoes a transformation into a system of ordinary differential equations (ODEs), allowing integration over time (Sabawi, et al. 2021 & Pirdawood, et al. 2022). It is noteworthy that radial basis functions (RBFs) possess a flexible shape parameter, influencing the accuracy of the solution and the conditions for the interpolation matrix of radial basis functions (Sadeeq, et al. 2022). The Implicit-Explicit Runge-Kutta (RK) scheme was implemented to address the ordinary differential equation system, as detailed in the research conducted by (Sabawi, et al. 2022). Furthermore, the solution for ordinary problems by implicit Runge-Kutta method have been introduced in the study carried out by (Sabawi, et al. 2023). From this research, we broaden the application of the RBF-Pseudo spectral method for obtaining approximate solution for the STO equation. Additionally, we will discritize STO equation within the bounds of $a \leq x \leq b$ and $0 \leq t \leq T_f$. Using the parameters and $x_i = x_{i-1} + h$,and $t_j = t_{j-1} + \tau$, for i from 0 to n_X, and j from 0 to m_T, with $h = (b-a)/n_X$ also $\tau = T_f/m_T$. The computer program Matlab 2021a will be employed to generate and visualize graphs illustrating the acquired solutions.

2. RBF-PSEUDO SPECTRAL METHOD

The core concept of the RBF-PS method centers on representing the solutions of partial differential equations (PDEs) through a collection of smooth basis functions denoted as B_j, where j takes values from 0 to n. These basis functions, exemplified by polynomials as discussed by (Fornberg, 1998), serve as a means to approximate the PDE solutions. The subsequent expressions represents the steps to approximate the solution of the Equation (1) by using the radial base function:

$$(\mathcal{A})_{ij} = \phi(\|x - x_j\|)\big|_{x=x_i},$$

$$v(x,t) \approx \hat{v}(x,t) = \sum_{j=0}^{n} c_{1j}\, \mathcal{B}_j(x), \tag{2}$$

where $\mathcal{B}_j(x)$ is represented as $\phi(\|x - x_j\|)$, with ϕ being a strictly positive definite radial basis function, and the norm $\|\cdot\|$ is the Euclidean norm which is utilized to represent the distance between x and x_j. In equation (2), the temporal aspect is ignored, meaning the unspecified functions c_j are time-dependent. Consequently, the sole remaining variable is the initial value variable, typically representing time in a physical scenario.

Radial Basis Functions (RBFs) are mathematical functions used in various fields such as interpolation, approximation, and machine learning. They are characterized by a central point or center and a radial distance from that center. The parameter ε, often referred to as the shape parameter or scale parameter, is a crucial aspect of RBFs, influencing their behavior and performance. This parameter plays a pivotal role in influencing the precision of a solution as well as the conditioning of the RBF interpolation matrix. Numerous researchers have delved into the behavior of this shape parameter in pursuit of achieving highly accurate solutions (Suárez and Morales, 2014). Let's take a closer look at the three popular RBFs and how the shape parameter ε affects them (Fasshauer, 2007):

- Multiquadric (MQ): $\phi(\rho) = \sqrt{\varepsilon^2 + \rho^2}$,

  The Multiquadric RBF is known for its smoothness and the ability to approximate functions with varying degrees of smoothness. The shape parameter ε controls the width of the basis function. A smaller ε results in a narrower basis function, which can lead to overfitting and oscillations in the interpolation, while a larger ε results in a broader basis function, which may oversmooth the data.

- Inverse Multiquadric (IMQ): $\phi(\rho) = \frac{1}{\sqrt{\varepsilon^2+\rho^2}}$;

  The Inverse Multiquadric RBF is similar to the Multiquadric but has a decaying behavior as ρ increases. The shape parameter ε plays a similar role as in the Multiquadric RBF, controlling the width of the basis function. Smaller ε values lead to narrower functions, and larger ε values lead to broader functions.

- Inverse quadric (IQ): $\phi(\rho) = \frac{1}{1+(\varepsilon\rho)^2}$.

  The Inverse Quadratic RBF is another popular choice, particularly in mesh-free methods like the Radial Basis Function Interpolation (RBF-FD). The shape parameter ε affects the steepness of the decay of the basis function as ρ increases. Smaller ε values result in a steeper decay, while larger ε values lead to a more gradual decay.

In general, selecting an appropriate ε is a critical step in using RBFs effectively. It should be chosen based on the characteristics of the data and the problem at hand. A small ε can provide a high degree of precision but may be sensitive to noise, while a large ε can provide smoother interpolations but may lose fine details in the data. The parameter ε, where $\varepsilon > 0$, serves as a structural parameter employed for adjusting the basis functions, while $\rho = \|x\|$ transforms into a radial variable. The choice of the specific RBF and the tuning of ε are important considerations when working with RBF-based methods, and they can significantly impact the accuracy and conditioning of the resulting interpolation or approximation. Further more details see (Saeed and Sadeeq 2017). Upon evaluating Eq. (2) at x_i within i from 0 to n, the following results will be derived:

$$\hat{v}(x,t) = \sum_{j=0}^{n} c_j\, \phi(\|x - x_j\|),$$

Alternatively, employing matrix notation:

$$V = \mathcal{A}C, \tag{3}$$

with $V = [\hat{v}(x_0,t), \dots, \hat{v}(x_0,t)]^T$, $(\mathcal{A})_{ij} = \phi(\|x - x_j\|)|_{x=x_i}$ and $C = [c_0, \dots, c_n]^T$.

We will calculate the derivative of $\hat{v}$ in equation (2), by taking the derivative of the base function:

$$\frac{\partial}{\partial x}\hat{v}(x,t) = \sum_{j=0}^{n} c_j\, \frac{d}{dx}\phi(\|x - x_j\|). \tag{4}$$

At the coordinates x_i on the grid, we can evaluate the Equation (4), resulting in:

$$\frac{\partial}{\partial x}\hat{v}(x,t)\Big|_{x=x_i} = \sum_{j=0}^{n} c_j\, \frac{d}{dx}\phi(\|x - x_j\|)|_{x=x_i}.$$

Alternatively, for being more compact we will write it as the matrix notation:

$$V_x = \mathcal{A}_x C, \tag{5}$$

with V and C both are introduced earlier, and $\mathcal{A}_x$ is specified as follows:

$$(\mathcal{A}_x)_{ij} = \frac{d}{dx}\phi(\|x - x_j\|)|_{x=x_i}.$$

Here are the procedures for solving the equation (3) in terms of C:

$$C = \mathcal{A}^{-1}V. \tag{6}$$

When we substitute the Equation (5) within the Equation (6), we will get:

$$V_x = \mathcal{A}_x\mathcal{A}^{-1}V.$$

Define D_x as the product of $\mathcal{A}_x$ and the inverse of $\mathcal{A}$. The preceding equation could be expressed in the following arrangement:

$$V_x = D_x V. \tag{7}$$

In particular, the matrix illustrating the differentiation of second derivative and third derivative will be presented as follows:

$$V_{xx} = D_{xx}V \text{ and } V_{xxx} = D_{xxx}V, \tag{8}$$

where $D_{xx} = \mathcal{A}_{xx}\mathcal{A}^{-1}$, $D_{xxx} = \mathcal{A}_{xxx}\mathcal{A}^{-1}$, $(\mathcal{A}_{xx})_{ij} = \frac{d^2}{dx^2}\phi(\|x - x_j\|)\big|_{x=x_i}$, and $(\mathcal{A}_{xxx})_{ij} = \frac{d^3}{dx^3}\phi(\|x - x_j\|)\big|_{x=x_i}$. The points x_i for i ranging from 0 to n, is employed to discretize the spatial domain for the purpose of solving equation (1). This process leads to:

$$v_t(x_i,t) = -3\beta v_x^2(x_i,t) - 3\beta v^2(x_i,t)v_x(x_i,t) - 3\beta v(x_i,t)v_{xx}(x_i,t) - \beta v_{xxx}(x_i,t).$$

We will write the proceeding equation in a more concise form:

$$\frac{dV}{dt} = -3\beta V_x^2 - 3\beta V^2 * V_x - 3\beta V * V_{xx} - \beta V_{xxx}, \tag{9}$$

In accordance with the earlier definition, V is as described before. Additionally, the symbol * denotes the component-wise multiplication of two vectors. When equations (7) and (8) are replaced in Equation (9), the result is:

$$\frac{dV}{dt} = -3\beta D_x V^2 - 3\beta V^2 * (D_x V) - 3\beta V * (D_{xx}V) - \beta D_{xxx}V. \tag{10}$$

To enhance conciseness, we will express (10) in the following manner:

$$\frac{dV}{dt} = \psi(t,V), \tag{11}$$

where

$$\psi(t,V) = -3\beta D_x V^2 - 3\beta V^2 * (D_x V) - 3\beta V * (D_{xx}V) - \beta D_{xxx}V.$$

Equation (1) has been transformed into the ODE with respect to the independent variable t, as determined by equation (11). We intend to employ the fourth-order Runge-Kutta technique (RK4M) to solve the Equation (11).

3. RUNGE-KUTTA METHOD

The family of techniques known as the Runge-Kutta method is commonly utilized for solving ordinary differential equations. The classical fourth-order Runge-Kutta method is presented as follows:

$$V^{(j+1)} = V^{(j)} + \frac{\tau}{6}(k_1 + 2k_2 + 2k_3 + k_4), \tag{12}$$

where,

$$k_1 = \psi(t_j, V^{(j)}),$$
$$k_2 = \psi\left(t_j + \frac{\tau}{2}, V^{(j)} + \frac{\tau k_1}{2}\right),$$
$$k_3 = \psi\left(t_j + \frac{\tau}{2}, V^{(j)} + \frac{\tau k_2}{2}\right),$$
$$k_4 = \psi(t_j + \tau, V^{(j)} + \tau k_3),$$
$$\text{and, } V^{(j)} = [\hat{v}(x_0, t_j), \dots, \hat{v}(x_n, t_j)]^T.$$

Hence, determining the approximated value of U at the point (x_i, t_j) involves assessing $V^{(j+1)}$ in Equation (12) successively for j from 0 to $m-1$. This process is applicable when the initial condition provides the value for $V^{(0)}$, allowing for the derivation of the approximate solution.

4. NUMERICAL EXAMPLES

The numerical investigations are conducted to validate the accuracy and efficiency of the method. Error norms are calculated to verify the validity of the approach. It is widely recognized that several factors, such as the selection of data points, the utilization of radial basis functions (RBF), the placement of center points, and the value of the shape parameter, influence the accuracy of the results. In the current study, we aim to solve Equation (1) the STO equation. In (Abdou, et al., 2020), we can find the exact solution which is represented as follows:

$$v(x,t) = \frac{1}{4}\tanh(x - \beta t) - \frac{1}{2}.$$

The initial conditions are set using the precise solution at $t = 0$. In this instance, a Multiquadric radial base function with $\varepsilon = 0.2$ will be employed. To assess the accuracy of the approaches, we utilize the absolute error L_{abs} and the maximum absolute error L_∞, as defined below:

$$L_{abs}(v) = |v(x_i,t) - V(x_i,t)|,$$
$$L_\infty(v) = \max_{0 \le i \le n} |v(x_i,t) - V(x_i,t)|, \ i = 0,1,\dots,n,$$

The graphical representation of the investigate findings is depicted within the Figures (1-4), while Table (1) and Table (2) represents the absolute and maximum absolute error.

Table 1. - The discrepancies in the solution for the STO equation at time t=10 with the value of the parameter β=0.001 are indicated by absolute errors.

x	$\lvert v(x,t)\rvert$ Exact	$\lvert V(x,t)\rvert$ IQ	$L_{abs}(v)$ IQ	$\lvert V(x,t)\rvert$ IMQ	$L_{abs}(v)$ IMQ	$\lvert V(x,t)\rvert$ MQ	$L_{abs}(v)$ MQ
−10	0.7500	0.7513	1.3159e-3	0.7509	9.0501e-4	0.7500	8.3097e-6
−8	0.7500	0.7504	3.8346e-4	0.7508	8.0057e-4	0.7500	3.3428e-5
−6	0.7500	0.7502	1.6791e-4	0.7505	4.6913e-4	0.7499	5.8392e-5
−4	0.7498	0.7498	4.3115e-6	0.7499	7.9422e-5	0.7498	5.8291e-5
−2	0.7412	0.7408	3.9834e-4	0.7407	4.7991e-4	0.7410	1.8352e-4
0	0.5025	0.5001	2.3940e-3	0.4997	2.7926e-3	0.5000	2.4658e-3
2	0.2592	0.2585	6.5432e-4	0.2589	3.2059e-4	0.2590	1.4550e-4
4	0.2502	0.2501	8.9264e-5	0.2500	1.3693e-4	0.2502	1.8045e-5
6	0.2500	0.2500	3.6818e-5	0.2499	1.0513e-4	0.2500	1.4775e-6
8	0.2500	0.2500	2.0163e-5	0.2499	8.3158e-5	0.2500	2.8529e-6
10	0.2500	0.2501	8.6641e-5	0.2499	7.5026e-5	0.2500	2.2860e-6

Table 2. The solution for the STO equation is characterized by its maximum absolute errors, denoted as L_∞.

	L_∞		
t	α =5e-5	α =4e-4	α =1e-3
0	0	0	0
1	1.2329e-5	9.8635e-5	2.4659e-4
2	2.4659e-5	1.9727e-4	4.9317e-4
3	3.6988e-5	2.9591e-4	7.3976e-4
4	4.9318e-5	3.9454e-4	9.8635e-4
5	6.1647e-5	4.9317e-4	1.2329e-3
6	7.3976e-5	5.9181e-4	1.4795e-3
7	8.6306e-5	6.9044e-4	1.7261e-3
8	9.8635e-5	7.8908e-4	1.9727e-3
9	1.1096e-4	8.8771e-4	2.2192e-3
10	1.2329e-4	9.8635e-4	2.4658e-3

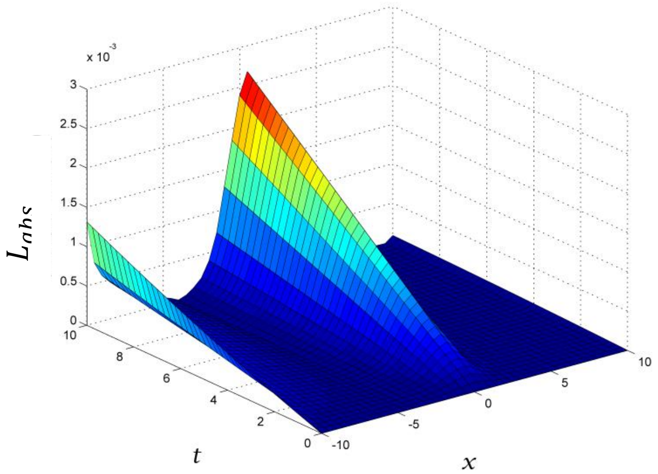

FIGURE 1. The absolute errors in solving the Sharma-Tasso-Olver equation using IQ are examined over the domain $a \le x \le b$, where $a = -10$ and $b = 10$, during the time interval $0 \le t \le \tau$. This analysis is conducted for the case where $\tau = 10, n = m = 40, \Delta x = (b-a)/n, \tau = \tau/m$, and $\beta = 0.001$.

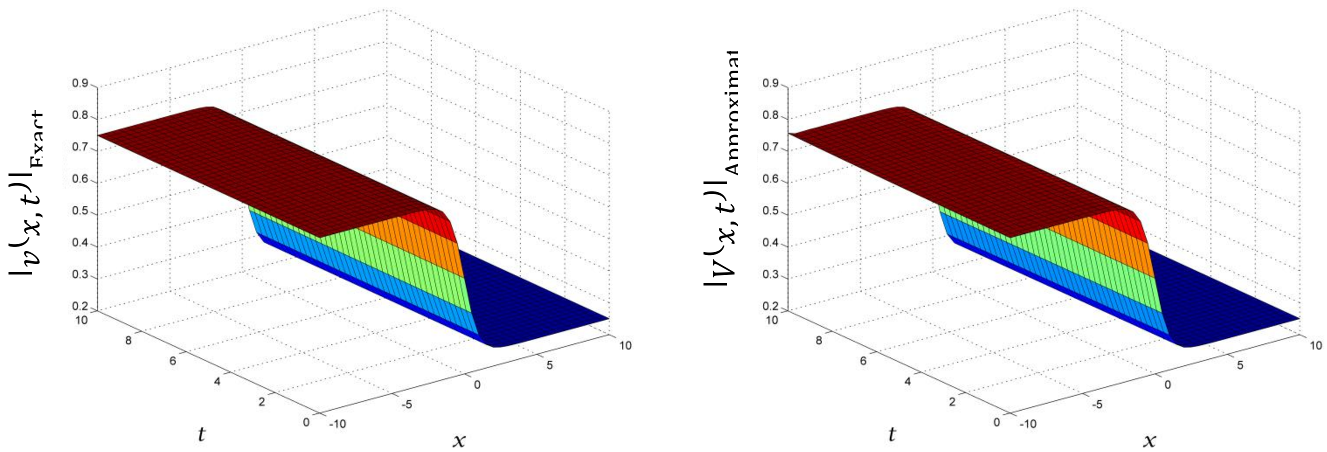

FIGURE 2. Comparing the absolute values of the exact and RBF-Pseudo spectral method approximations for the Sharma-Tasso-Olver equation. Parameters and the x-domain match those in Figure 1.

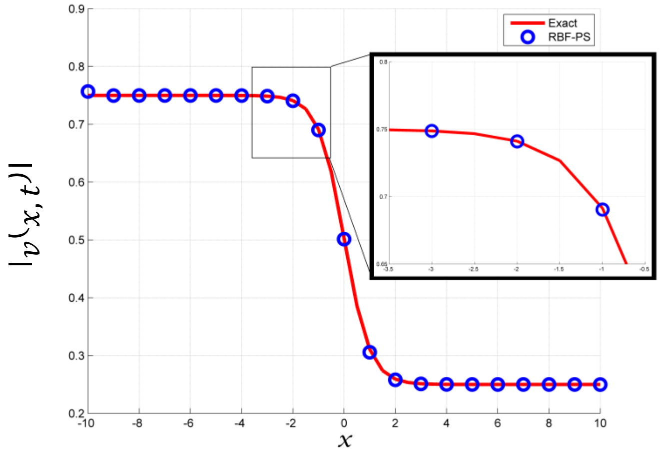

FIGURE 3. Comparing approximated and exact solutions for v at t=5, with x-domain and parameters matching Figure 1.

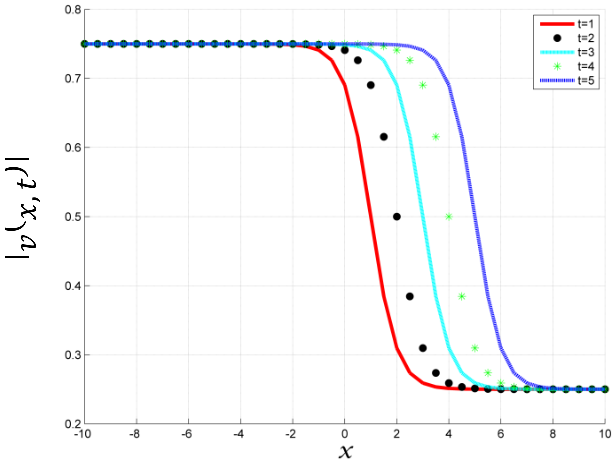

FIGURE 4. The Variation in $v(x,t)$ at different time instances in relation to the standardized propagation position x is examined, with $\beta = 1$.

5. CONCLUSION

We successfully employed a combination of the radial basis function pseudo spectral technique for spatial calculations and the 4th order Runge-Kutta method for temporal calculations to numerically solve the Sharma-Tasso-Olver equation (1). In our investigation, we evaluated three commonly used radial basis functions, namely multiquadric (MQ), inverse multiquadric (IMQ), and inverse quadric (IQ). Our findings, as depicted in Table 1, indicate that, among these radial basis functions, multiquadric outperforms the others in terms of accuracy when comparing the exact solution with the approximate one. The obtained approximate results underscore the effectiveness and success of this method in generating numerical solutions for the model. The outcomes produced using this method demonstrate an exceptional level of agreement with the exact solutions, affirming its robustness in tackling the Sharma-Tasso-Olver equation across various consequences. Particularly, this method exhibits superior performance for certain parameter value.

REFERENCES

[1] Wazwaz, A.M., 2007. New solitons and kinks solutions to the Sharma–Tasso–Olver equation. Applied Mathematics and Computation, 188(2), pp.1205-1213. https://doi.org/10.1016/j.amc.2006.10.075.

[2] He, Y., Li, S. and Long, Y., 2013. Exact solutions to the sharma-tasso-olver equation by using improved-expansion method. Journal of Applied Mathematics, 2013. http://dx.doi.org/10.1155/2013/247234.

[3] Uddin, M.H., Khan, M.A., Akbar, M.A. and Haque, M.A., 2019. Multi-solitary wave solutions to the general time fractional Sharma–Tasso–Olver equation and the time fractional Cahn–Allen equation. Arab Journal of Basic and Applied Sciences, 26(1), pp.193-201. https://doi.org/10.1080/25765299.2019.1599207.

[4] Abdou, M.A., Ouahid, L., Owyed, S., Abdel-Baset, A.M., Inc, M., Akinlar, M.A. and Chu, Y.M., 2020. Explicit solutions to the Sharma-Tasso-Olver equation. AIMS Mathematics, 5(6), pp.7272-7284. https://doi.org/10.3934/math.2020465.

[5] Kang, Z., Xia, T. and Ma, W., 2019, April. Abundant multiwave solutions to the (3+ 1)-dimensional Sharma-Tasso-Olver-like equation. In Proc. Rom. Acad. Ser. A (Vol. 20, No. 2, pp. 115-122).

[6] Sabawi, Y.A., Pirdawood, M.A. and Sadeeq, M.I., 2021, September. A compact fourth-order implicit-explicit Runge-Kutta type method for solving diffusive Lotka–Volterra system. In Journal of Physics: Conference Series (Vol. 1999, No. 1, p. 012103). IOP Publishing. https://doi.org/10.1088/1742-6596/1999/1/012103.

[7] Pirdawood, M.A. and Sabawi, Y.A., 2021, September. High-order solution of Generalized Burgers–Fisher Equation using compact finite difference and DIRK methods. In Journal of Physics: Conference Series (Vol. 1999, No. 1, p. 012088). IOP Publishing. https://doi.org/10.1088/1742-6596/1999/1/012088.

[8] Zhou, Y. and Zhuang, J., 2022. Dynamics and Exact Traveling Wave Solutions of the Sharma–Tasso–Olver–Burgers Equation. Symmetry, 14(7), p.1468. https://doi.org/10.3390/sym14071468.

[9] Sheikh, M.A.N., Taher, M.A., Hossain, M.M. and Akter, S., 2023. Variable coefficient exact solution of Sharma–Tasso–Olver model by enhanced modified simple equation method. Partial Differential Equations in Applied Mathematics, p.100527. https://doi.org/10.1016/j.padiff.2023.100527.

[10] Buhmann, M.D., 2000. Radial basis functions. Acta numerica, 9, pp.1-38.

[11] Sabawi, Y.A., Pirdawood, M.A. and Khalaf, A.D., 2021, September. Semi-implicit and explicit runge kutta methods for stiff ordinary differential equations. In Journal of physics: Conference series (Vol. 1999, No. 1, p. 012100). IOP Publishing. https://doi.org/10.1088/1742-6596/1999/1/012100.

[12] Pirdawood, M.A., Rasool, H.M., Sabawi, Y.A. and Azeez, B.F., 2022. Mathematical modeling and analysis for COVID-19 model by using implicit-explicit Rung-Kutta methods. Academic Journal of Nawroz University, 11(3), pp.65-73. https://doi.org/10.25007/ajnu.v11n3a1244.

[13] SADEEQ, M.I., OMAR, F.M. and PIRDAWOOD, M.A., 2022. Numerical solution of Hirota-Satsuma coupled Kdv system By Rbf-Ps method. Journal of Duhok University, 25(2), pp.164-175. https://doi.org/10.26682/sjuod.2022.25.2.15

[14] Sabawi, Y.A., Pirdawood, M.A., Rasool, H.M. and Ibrahim, S., 2022, May. Model Reduction and Implicit–Explicit Runge–Kutta Schemes for Nonlinear Stiff Initial-Value Problems. In International Conference on Mathematics and Computations (pp. 107-122). Singapore: Springer Nature Singapore. https://doi.org/10.1007/978-981-99-0447-1_9.

[15] Sabawi, Y.A., Pirdawood, M.A. and Khalaf, A.D., 2023, February. Signal diagonally implicit Runge Kutta (SDIRK) methods for solving stiff ordinary problems. In AIP Conference Proceedings (Vol. 2457, No. 1). AIP Publishing. https://doi.org/10.1063/5.0118644.

[16] Fornberg, B., 1998. A practical guide to pseudospectral methods (No. 1). Cambridge university press.Suárez, P.U. and Morales, J.H., 2014. Numerical solutions of two-way propagation of nonlinear dispersive waves using radial basis functions. International Journal of Partial Differential Equations, 2014.

[17] Fasshauer, G.E., 2007. Meshfree approximation methods with MATLAB (Vol. 6). World Scientific.

[18] Saeed, R.K. and Sadeeq, M.I., 2017. Radial Basis Function-Pseudospectral Method for Solving Non-Linear Whitham-Broer-Kaup Model. Sohag Journal of Mathematics, 4(1), pp.13-18. https://doi.org/10.18576/sjm/040103.